Mechanism of Photooxidation of Trichloroethylene on TiO_2: Detection of Intermediates by Infrared Spectroscopy

Jingfu Fan and John T. Yates, Jr.*

Contribution from the Surface Science Center, Department of Chemistry, University of Pittsburgh, Pittsburgh, Pennsylvania 15260

Received June 30, 1995[⊗]

Abstract: The photooxidation of trichloroethylene (TCE) on TiO_2 has been investigated using infrared spectroscopy for kinetic studies of the production of intermediate species and for investigation of the reaction mechanism. Trichloroethylene is oxidized by chemisorbed molecular O_2 when TiO_2 band gap radiation ($h\nu > 3.1 \pm 0.1$ eV) is incident. An intermediate species, dichloroacetyl chloride, HCl_2CCOCl, was identified. At 300 K, Cl_2CO, CO, CO_2, HCl, and H_2O are final photooxidation products. At 473 K, Cl_2CO undergoes a thermal side reaction on TiO_2 to produce $Cl_2C{=}CCl_2$. Studies in which oxygen-labeled H_2O was present indicated no incorporation of the oxygen label into any of the intermediates, showing that the $OH^{\bullet}$ driven oxidation mechanism proposed by others is not operative. At 150 K, TCE blocks TiO_2 sites, significantly retarding O_2 adsorption and slowing the photooxidation reaction.

I. Introduction

The use of TiO_2 as a photocatalyst for environmental cleanup is of great current interest since TiO_2 is stable and inexpensive and has a UV absorption partially overlapping the solar spectrum.[1,2] Electron-hole pairs are photolytically generated by exciting the TiO_2 semiconductor with UV light:

$$TiO_2 + h\nu \rightarrow e^- + h^+ \qquad (1)$$

It has been postulated that the holes which diffuse to the TiO_2 surface react with surface OH groups. The subsequently formed OH radicals ($OH^{\bullet}$) are proposed to be oxidizing agents.[3] In this OH radical model, in order to prevent recombination of the holes with electrons, it was postulated that acceptor molecules are needed to trap the electrons to prevent electron-hole pair recombination in the bulk and on the TiO_2 surface.[4] Oxygen is an electron-trapping molecule and it was found to be indispensable for photooxidation reactions.[5−8] However, in a study of the photooxidation of methyl chloride on single crystal TiO_2(110), Lu, Linsebigler, and Yates[5] found that while both surface defect sites and oxygen adsorption are necessary for the photooxidation reaction to occur, the adsorbed oxygen is the actual oxidizing agent. Other studies also suggest that the role of oxygen may not just be limited to electron-trapping.[8−11] In this paper, the photooxidation of trichloroethylene (TCE) on powdered TiO_2 was studied. The purpose of this study is to examine the reaction mechanism of the photooxidation of TCE which is currently under discussion.[12−17]

There has been active interest in the photooxidation of TCE using TiO_2.[12−17] As a widely used solvent in industrial processes, TCE is the most common and abundant pollutant in ground water in the United States.[18] Since oxidation rates are typically orders of magnitude higher in the gas phase than in aqueous solution, an approach that strips the TCE from water and then carries out the UV photooxidation in the resulting air stream is being considered.[13,19] Thus, the study of the TiO_2 photocatalyzed oxidation of TCE is practically useful. Previous studies[14−16] have shown that a significant amount of toxic byproducts (chlorinated molecules) were formed in the photooxidation of TCE using TiO_2 in both aqueous solution and the gas phase. In studies of TCE photooxidation on TiO_2 in aqueous suspension, Pruden and Ollis[20] suggested that hydroxyl radicals initiate the reaction, and that dichloroacetaldehyde (DCAAD) is an intermediate. Glaze, Kenneke, and Ferry[16] argued that in addition to the hydroxyl radical initiated oxidative reaction channel, a parallel reductive pathway, involving the conduction band electrons of TiO_2, also plays an important role. This reductive pathway yields dichloroacetaldehyde and dichloroacetic acid (DCAA) as initial products from TCE. In studies of the TiO_2 photocatalyzed gaseous TCE oxidation, Anderson,

[⊗] Abstract published in *Advance ACS Abstracts,* May 1, 1996.

(1) Linsebiger, A. L.; Lu, G.; Yates, J. T., Jr. *Chem. Rev.* **1995**, *95*, 735.
(2) Wold, A. *Chem. Mater.* **1993**, *5*, 280.
(3) Jaeger, C. D.; Bard, A. J. *J. Phys. Chem.* **1979**, *83*, 3146.
(4) Gerischer, H.; Heller, A. *J. Phys. Chem.* **1991**, *95*, 5261.
(5) Lu, G.; Linsebigler, A.; Yates, J. T., Jr. *J. Phys. Chem.* **1995**, *99*, 7626.
(6) Fox, M. A.; Dulay, M. T. *Chem. Rev.* **1993**, *93*, 341.
(7) Wang, C.; Heller, A.; Gerischer, H. *J. Am. Chem. Soc.* **1992**, *114*, 5230.
(8) Wong, J. C. S.; Linsebigler, A.; Lu, G.; Fan, J.; Yates, J. T., Jr. *J. Phys. Chem.* **1995**, *99*, 335.
(9) Hoffmann, M. R.; Martin, S. T.; Choi, W.; Bahnemann, D. W. *Chem. Rev.* **1995**, *95*, 69.
(10) Hoffmann, A. J.; Carraway, E. R.; Hoffmann, M. R. *Environ. Sci. Technol.* **1994**, *28*, 776.
(11) Stafford, U.; Gray, K. A.; Kamat, P. V.; Varma, A. *Chem. Phys. Lett.* **1993**, 55.
(12) Phillips, L. A.; Raupp, G. B. *J. Mol. Catal.* **1992**, *77*, 297.
(13) Dibble, L. A.; Raupp, G. B. *Environ. Sci. Technol.* **1992**, *26*, 492.
(14) Nimlos, M. R.; Jacoby, W. A.; Blake, D. M.; Milne, T. A. *Environ. Sci. Technol.* **1993**, *27*, 732.
(15) Holden, W.; Marcellino, A.; Valic, D.; Weedon, A. C. In *Photocatalytic Purification and Treatment of Water and Air*; Ollis, D. F., Al-Ekabi, H., Eds.; Elsevier Science Publisher: New York, 1993; p 393.
(16) Glaze, W. H.; Kenneke, J. F.; Ferry, J. L. *Environ. Sci. Technol.* **1993**, *27*, 177.
(17) Zhang, Y.; Crittenden, J. C.; Hand, D. W.; Perram, D. C. *Environ. Sci. Technol.* **1994**, *28*, 435.
(18) Dyksen, J. E.; Hess, A. F., III. *J. AWWA* **1982**, *August*, 394.
(19) (a) Blystone, P. G.; Johnson, M. D.; Haag, W. R. Air & Waste Management Association, 85th Annual Meeting, June 21, 1992, Kansas City, MO. (b) Blystone, P. G.; Johnson, M. D.; Haag, W. R.; Daley, P. F. Advanced Ultraviolet Flash Lamps for the Destruction of Organic Contaminants in Air. In *Emerging Technologies In Hazardous Waste Management III*; Tedder, D. W., Pohland, F. G., Eds.; ACS Symposium Series, 518; American Chemical Society: Washington, DC, 1993; p 380.
(20) Pruden, A. L.; Ollis, D. F. *J. Catal.* **1983**, *82*, 404.

S0002-7863(95)02155-X CCC: $12.00

Nishida, and March[21] proposed a mechanism involving hydroxyl radicals and monochloroacetate as intermediates. Phillips and Raupp[12] suggested that hydroxyl radical or hydroperoxide radical initialized the reaction and involved dichloroacetaldehyde as an intermediate. In contrast, Nimlos, Jacoby, Blake, and Milne[14,22] suggested that TCE is oxidized in chain reactions initiated by chlorine atoms. Thus, various mechanisms are currently proposed for TCE photooxidation on the TiO_2 surface.

In this paper, the photooxidation of gaseous TCE was performed on a dehydroxylated TiO_2 sample in a controlled fashion. The use of dehydroxylated TiO_2 established a condition that the amount of surface hydroxyl groups on the TiO_2 surface is small,[23] and the possibility of both photooxidation reaction and gas−solid isotopic exchange via hydroxyl groups was minimized.[24,25] We then compared these results with experiments where significant amounts of water were present. We studied photooxidation reactions at 300 K where surface sites are accessible to gaseous TCE, water, and oxygen molecules. We also examined the photooxidation of TCE on TiO_2 surfaces at 150 K. Since TCE was adsorbed to high coverage on the TiO_2 surface at 150 K, the active surface sites were less accessible to oxygen under these conditions. We also investigated the thermal and photooxidation reactions at 473 K, where a thermal side reaction which does not take place at 300 K was observed.[26] Fourier Transform Transmission Infrared (FTIR) analysis and isotopic labeling methods were used to determine the reactions products and kinetics of the photooxidation by spectroscopic analysis in the gas phase and on the TiO_2 surfaces.

II. Experimental Section

Experiments were carried out in an infrared cell capable of operation at sample temperatures from 150 to 1500 K. The internal volume of the cell is 385 cm^3. A detailed description of this cell can be found elsewhere.[8,27] In brief, the TiO_2 particles were supported on a tungsten grid using a spraying technique developed in this laboratory. The temperature of the TiO_2 deposit could be very easily adjusted between 150 and 1500 K using electrical heating of the grid and a programmable controller operating off of feedback from a thermocouple welded to the grid. The reaction cell was set up so that infrared spectra of the TiO_2 surface and of the gaseous species inside the cell could be measured alternatively. KBr single crystals were used as infrared windows and were sealed by concentric viton O-rings. The window seals were differentially pumped by a mechanical pump. The system was pumped by both turbomolecular and ion pumps and a base pressure better than 1×10^{-8} Torr was achieved routinely. The pressure measurements were carried out using a capacitance manometer (Baratron, 116A, MKS) or using the ion current drawn by the ion pump (Varian, 921-0062). The analytical system we used in this study consists of a FTIR spectrometer (RS-1, Mattson), a gas chromatograph (5890 series II, Hewlett Packard, column DB-624, FID detector), and a quadrupole mass spectrometer (M100M, Dycor Electronics Inc.).

The $CHClCCl_2$ (TCE) was purchased from Aldrich with a quoted minimum purity of 99+%. The compound was transferred under nitrogen into a glass storage bulb after being passed through an alumina column to remove the small amount of added stabilizer. TCE was then further purified with several freeze−pump−thaw cycles using liquid nitrogen and ethanol−liquid nitrogen baths. The oxygen was obtained from Matheson Gas Products with a quoted purity of 99.999%. The oxygen-18 enriched oxygen gas was obtained from ICON Services Inc. with a quoted isotopic purity of 96 atom %. The TiO_2 powder (P25) was purchased from Degussa. Ultrapure H_2O was prepared by ion-exchange and distillation. The following procedure was followed to ensure a homogeneous mixture of TCE and oxygen inside the infrared reaction cell: TCE of the desired quantity was first introduced to the reaction cell and condensed on the TiO_2 sample holder using liquid nitrogen. Oxygen was then introduced and the TCE was allowed to evaporate back into the gas phase by warming the sample holder and TiO_2 to room temperature.

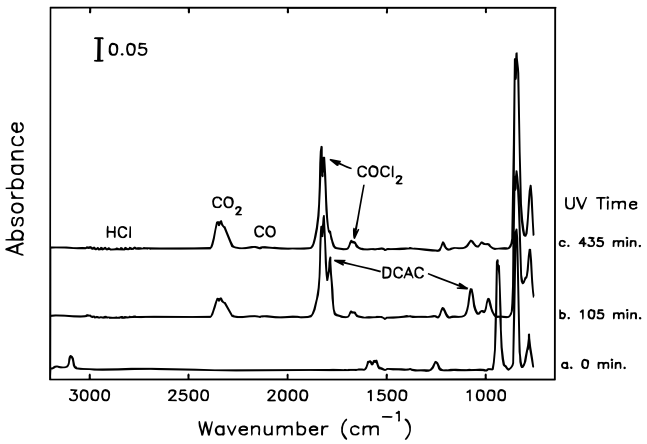

Figure 1. Gas-phase infrared spectra for $Cl_2C{=}CHCl$ (TCE) photooxidation at 300 K: (a) before irradiation; (b) after 105 min of UV irradiation; and (c) after 435 min of UV irradiation. $\lambda = 325 \pm 50$ nm.

The P25 TiO_2 is reported to have 70% anatase and 30% rutile structures, and a surface area of ∼50 m^2/g at room temperature.[28] Before any experiments, the TiO_2 was pretreated at 473 K in vacuum overnight to remove any adsorbed water, and then at ∼623 K for more than 2 h to remove the majority of surface hydroxyl groups and organic contamination.[23] The amount of TiO_2 used in an experiment was ∼30 mg sprayed over a grid of ∼5.2 cm^2 area. The TiO_2 weight could be visually estimated during the sample preparation[27] and accurately determined after performing the oxidation reactions.

The UV source is a 350-W high-pressure mercury arc lamp (Oriel Corp.). A 325 ± 50 nm bandpass filter was used in all the experiments except for the photothreshold measurements. The photon flux at 325 nm is 1×10^{17} photons cm^{-2} s^{-1} with an absolute accuracy of ±10% in our measurement using a EG&G (HUV-4000B) photodiode.[29] A series of interference filters (Oriel Corp., ∼10 nm width) in the range of 200 to 500 nm was used in our laboratory for the UV photon-energy dependent study and the photon fluxes at each wavelength were determined with the photodiode. A manual shutter was also installed to accurately control the UV exposure time. In all experiments, 4 cm^{-1} spectral resolution and signal averaging of 100 scans were used in the infrared measurements.

III. Results

A. Room Temperature Gas-Phase Photooxidation. Figure 1 shows the gas-phase infrared spectra taken at three different reaction stages of TCE oxidation on TiO_2 at 300 K. Before reaction, Figure 1a shows a typical gaseous TCE infrared spectrum; the positions and assignments of the observed infrared bands are summarized in Table 1. After mixing ∼4 Torr of TCE and ∼10 Torr of oxygen in the cell and irradiating with UV light for 105 min, we observed that the trichloroethylene (TCE) gas-phase spectral features disappeared completely. Dichloroacetyl chloride (DCAC, $CHCl_2COCl$), CO, phosgene

(21) Anderson, M. A.; Yamazaki-Nishida, S.; Cervera-March, S. In *Photocatalytic Purification and Treatment of Water and Air*; Ollis, D. F., Al-Ekabi, H., Eds.; Elsevier Science Publisher: New York, 1993; p 405.
(22) Nimlos, M. R.; Jacoby, W. A.; Blake, D. M.; Milne, T. A. In *Photocatalytic Purification and Treatment of Water and Air*; Ollis, D. F., Al-Ekabi, H., Eds.; Elsevier Science Publisher: New York, 1993; p 387.
(23) Fan, J.; Yates, J. T., Jr. *J. Phys. Chem.* **1994**, *98*, 10621.
(24) Sato, S. *J. Phys. Chem.* **1987**, *91*, 2895.
(25) Sato, S. *Langmuir* **1988**, *4*, 1156.
(26) Lu, G.; Linsebigler, A.; Yates, J. T., Jr. *J. Phys. Chem.* **1994**, *98*, 11733 and references therein.
(27) Basu, P.; Ballinger, T. H.; Yates, J. T., Jr. *Rev. Sci. Instrum.* **1988**, *59*, 1321.
(28) Highly Dispersed Metallic Oxides Produced by Aerosil Process; Degussa Technical Bulletin Pigments No. 56, 1990, p 13.
(29) Hanley, L.; Guo, X.; Yates, J. T., Jr. *J. Chem. Phys.* **1989**, *91*, 7220.
(30) Tanaka, K.; Blyholder, G. *J. Phys. Chem.* **1972**, *76*, 1807.

Table 1. Assignments of the Observed Infrared Frequencies in the Photooxidation of TCE at 300 K

compds	infrared freq (cm^{-1})
$Cl_2C{=}CHCl$ (g) (TCE)[12]	3169 (C−H); 3099 (C−H); 1586, 1555 (C=C); 1251 (CH−Cl); 944, 783, 631 (C−Cl); 848 (C−H)
$Cl_2CH{-}COCl$ (g) (DCAC)[45]	1820, 1788 ($C{=}^{16}O$); 1225 (C−H); 1076, 989 (C−C); 800, 741 ($C{-}Cl_2$); 1783, 1751 ($C{=}^{18}O$)
$COCl_2$ (g)[46]	1833, 1820 ($C{=}^{16}O$); 1682 [2($C{-}Cl_2$)]; 852, 662 ($C{-}Cl_2$); 1793, 1783 ($C{=}^{18}O$)
CO_2 (g)[33]	2349 ($^{16}O{=}C{=}^{16}O$); 2331 ($^{18}O{=}C{=}^{18}O$)
CO (g)	2143 ($C{\equiv}^{16}O$); 2091 ($C{\equiv}^{18}O$)
$CHCl_3$ (g)	1219, 773

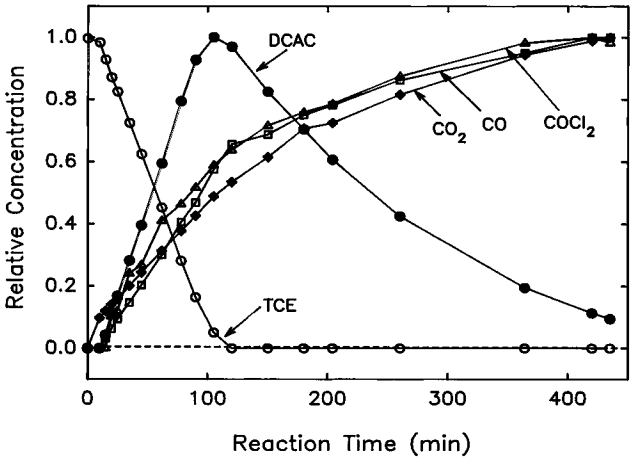

Figure 2. Kinetics for $Cl_2C{=}CHCl$ (TCE) oxidation at room temperature. For easy comparison, only normalized gas-phase concentrations are shown.

(Cl_2CO), CO_2, and HCl spectral features appeared in the infrared spectrum as revealed in Figure 1b. The assignments of these newly formed species are also summarized in Table 1. After extensive UV irradiation (435 min), Figure 1c shows that most of the DCAC had converted to CO_2, phosgene, CO, and HCl. The kinetics of the TCE oxidation reaction are plotted in Figure 2. The measurements in Figure 2 were obtained from gas-phase infrared band intensities and were normalized for easy comparison. The concentrations for CO_2, CO, TCE, DCAC, and $COCl_2$ were based on their infrared bands at 2349, 2143, 1555, 1077, and 1682 cm^{-1}, respectively. Figure 2 clearly shows that DCAC, as a gas-phase reaction intermediate, is further converted to CO_2, CO, and phosgene. Also, the maximum concentration for DCAC occurred at the time when TCE was completely consumed, an indication that DCAC was directly formed from TCE. The constant slope for the TCE consumption curve before 100 min suggests that the rate of TCE oxidation remained relatively unchanged during most of the reaction. This may suggest that the photooxidation reaction follows zero-order kinetics with TCE.[30] The kinetics for HCl formation are not plotted in Figure 2 due to difficulties in performing a quantitative analysis of the intensity of its rotational bands at ~2900 cm^{-1}. The change in infrared absorption intensities for DCAC was consistent for the bands at 1788, 1077, and 741 cm^{-1}, which follow the trend shown in Figure 2 for DCAC. However, this is not the case for bands at 1225 and 800 cm^{-1}. Careful analysis shows that each of the two bands actually was a superimposition of two bands. In Figure 1b, we observed that the band centered at 1225 cm^{-1} has a shoulder at 1210 cm^{-1}, and the band centered at 800 cm^{-1} has a shoulder at 780 cm^{-1}. In Figure 1c, the band originally at 1225 cm^{-1} was shifted to 1219 cm^{-1}, and that originally at 800 cm^{-1} was shifted to 773 cm^{-1}. Since

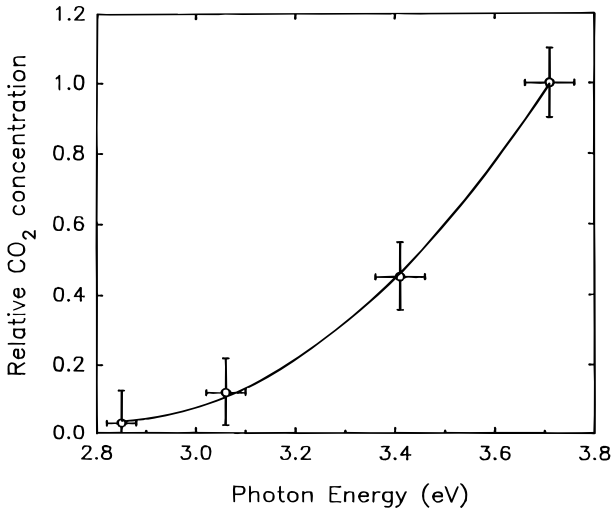

Figure 3. Energy dependence of the calibrated and normalized photooxidation yield for TCE oxidation at 300 K. The CO_2 yields are obtained from infrared band intensities. The reaction time is 300 min; initial oxygen pressure is ~4 Torr; initial TCE pressure is ~2 Torr.

most of the DCAC was already oxidized in Figure 1c, the remaining peaks at 1219 and 773 cm^{-1} must be due to an additional species. These two peaks are assigned to $CHCl_3$ based on standard spectra. Thus, the detected products from TCE photooxidation on TiO_2 are CO_2, $COCl_2$, CO, HCl, and a trace of $CHCl_3$. Although our experiment was performed in a closed reaction cell, the reaction kinetics and reaction products as detected by infrared measurements are in general agreement with that reported by Nimlos et al.[14,22] and by Holden et al.[15] in their studies of TCE photooxidation in a flowing air stream. Closely related intermediates and final products were also reported for photooxidation of TCE in aqueous solution.[16] In a separate experiment, we found that DCAC underwent photooxidation in oxygen on TiO_2, forming CO_2, CO, $COCl_2$, and HCl as products. This further suggested that DCAC was an intermediate in the photooxidation of TCE. Our carbon balance analysis based on infrared absorption calibrations using pure CO_2 and CO shows ~67 mol % CO_2 and ~14 mol % CO in the final product mixture after extended UV exposure. The $COCl_2$ and $CHCl_3$ yield therefore corresponds to 19 mol % by difference. Assuming as an order of magnitude that each surface site on TiO_2 is of 10 $Å^2$ area, the complete conversion of TCE to oxidation products in these experiments involves about 3−4 primary molecular oxidation events per surface site. The reaction rate is controlled by O_2 activation at vacancy defect sites (as was determined on single-crystal $TiO_2(110)$[5]) and if these sites occupy ~10% of the surface, then 30−40 primary molecular oxidation events occur per active defect site at complete conversion.

A separate experiment was done to look at the possibility of thermal reactions inside the reaction cell which might occur in the dark. In this experiment, the UV light was turned off after 30 min of total UV irradiation and an infrared spectrum was obtained just before the light was turned off. After 1 h another infrared spectrum was recorded. No change in the TCE absorption was observed in these two infrared spectra. However, the photooxidation was observed to resume after the UV light was turned back on.

Figure 3 shows the result of TCE oxidation under UV irradiation with photon energies of 2.85 ± 0.03, 3.06 ± 0.04, 3.41 ± 0.05, and 3.71 ± 0.05 eV. All the experiments in Figure 3 were performed at room temperature for 300 min, using ~2 Torr of TCE and ~4 Torr of oxygen. The yields of CO_2 are

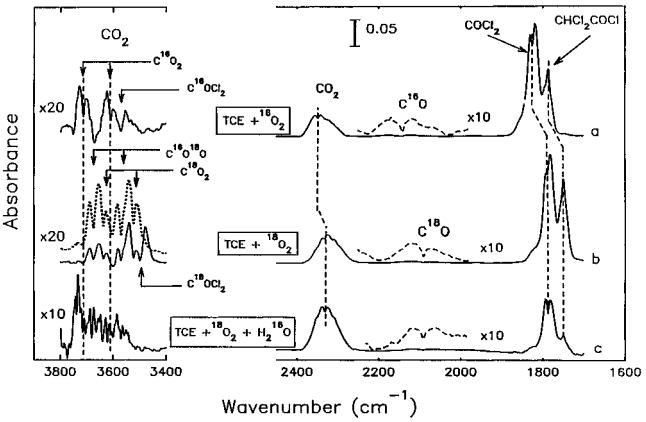

Figure 4. Isotopic shifts for the frequencies of carbonyl stretches of DCAC, phosgene, CO, and CO_2 during TCE oxidation at 300 K in $^{16}O_2$, $^{18}O_2$ with and without the presence of $H_2{}^{16}O$. $P_{H_2O} = \sim 10$ Torr. (See text for details.)

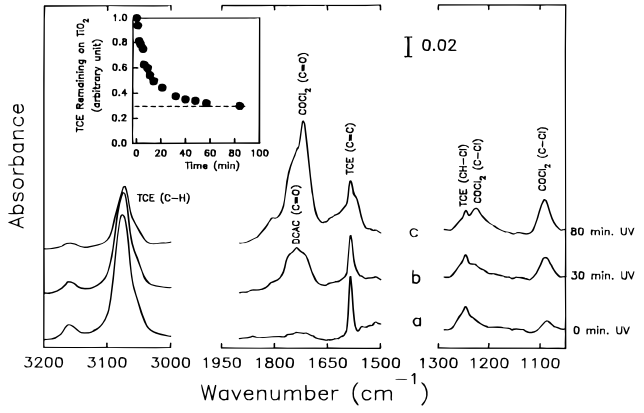

Figure 5. Development of infrared spectra of photolytically generated species on the TiO_2 surface during TCE oxidiation at 150 K: (a) before UV irradiation; (b) after 30 min of UV irradiation; and (c) after 80 min of UV irradiation. The insert shows the change of adsorbed TCE concentration on the TiO_2 surface.

based on the IR band intensities and are normalized to the absolute photon-fluxes through the band pass filters measured before and after each experiment. Figure 3 shows that the CO_2 production is very low below a photon energy of 3.1 eV. The threshold near 3.1 ± 0.1 eV corresponds to the band gap of rutile and anatase TiO_2.[31,32] The rate of CO_2 production increases significantly for photon energies above the band gap. This result is consistent with other studies reported for gas-phase and aqueous-solution oxidation of TCE in which control experiments showed no photooxidation of TCE in the absence of TiO_2 particles under UV irradiation ($\lambda > 290$ nm).[14−16]

The increase in the reaction rate with increasing UV photon energy above the threshold energy at ∼3.1 eV shown in Figure 3 was also observed in other studies on single-crystal TiO_2-(110).[5] Since O_2 is the oxidation agent, the differences in reaction rates may be attributed to differences in O_2-TiO_2 excitation. As the photon energy increases, more energetic electrons will be produced and will tunnel into a broadened acceptor band in adsorbed O_2, giving an increase in reaction rate over a wide range of photon energy above 3.1 eV, as observed.

Figure 4 shows the IR spectrum for TCE oxidation on TiO_2 using $^{18}O_2$ at 300 K. The results obtained using oxygen-16 are also shown in Figure 4a for comparison. In Figure 4a, the three infrared bands at ∼1800 cm^{-1} correspond to the carbonyl stretches of DCAC and phosgene. Upon using oxygen-18, Figure 4b shows that all the carbonyl stretching frequencies were shifted down by ∼39 cm^{-1}. The CO stretch at ∼2100 cm^{-1} for carbon monoxide was also shifted down ∼52 cm^{-1}. The fact that only oxygen-18 is incorporated into DCAC, phosgene, and CO indicates that only the oxygen from the gas phase is involved in the oxidation of TCE to DCAC, phosgene, and CO. The isotopic content of CO_2 is not easily discerned from the CO_2 stretching frequencies at ∼2300 cm^{-1} due to fairly small isotopic shifts and overlapping of multiple bands. However, the overtone and combination bands for the CO_2 molecule containing different oxygen isotopes at ∼3700 cm^{-1} are well separated and well documented.[33−35] Observation of the CO_2 missing spectral branches provides the clearest information. Figure 4a shows that only two missing branches at 3713, 3610 cm^{-1} are observed for $C^{16}O_2$, while Figure 4b clearly shows that missing branches at 3675, 3572 cm^{-1} and 3637, 3524 cm^{-1} are observed for $C^{16}O^{18}O$ and $C^{18}O_2$, respectively. The observation of both isotopic oxygen-16 and oxygen-18 in the CO_2 product in Figure 4b indicates that oxygen from both lattice TiO_2 and gas-phase O_2 is involved in the final oxidation to CO_2, since TiO_2 is the only possible source of oxygen-16 and $^{18}O_2$ is the only possible source of oxygen-18. The extra valleys at 3568 cm^{-1} in Figure 4a and 3500 cm^{-1} in Figure 4b are due to DCAC and phosgene products as shown by a separate calibration experiment. In this experiment, when the DCAC was all consumed and $COCl_2$ was thermally reacted at 473 K (see section III.C for details), we observed that the valley features at 3568 and 3500 cm^{-1} disappear while the other features of CO_2 remain as shown in the spectrum plotted in the dashed line in Figure 4b. Figure 4c shows the infrared spectra obtained during TCE oxidation with oxygen-18 in the presence of $H_2{}^{16}O$. Figure 4c demonstrates that only oxygen-18 is incorporated into DCAC, $COCl_2$, and CO based upon the positions of the carbonyl stretching frequencies for those molecules using the same arguments above when discussing Figures 4a and 4b. This indicates that the molecular oxygen involvement in the oxidation reaction is not changed by the presence of water vapor, and that oxygen-16 from $H_2{}^{16}O$ is not incorporated in the photo-oxidation products. Unfortunately, the overtone region for CO_2 in Figure 4c cannot be used to determine the isotopic content of CO_2 in the experiment done in the presence of water due to the interference from the OH stretch modes of water. However, by comparing the spectra in Figure 4a−c, the very similar spectral profiles of the CO_2 stretch mode at ∼2300 cm^{-1} in Figures 4b and 4c suggest that the isotopic content of carbon dioxide in Figure 4c in the presence of water is mostly $C^{18}O^{16}O$ and $C^{18}O_2$ as was also found in the absence of $H_2{}^{16}O$. Figure 4c, compared to Figure 4b, shows that in the presence of H_2O, the yield of CO_2 is increased and the yield of DCAC is decreased. This is probably due to the hydrolysis of DCAC and $COCl_2$ to produce CO_2, HCl, and dichloroacetic acid.[19,36]

B. Photooxidation on TiO_2 at 150 K. Figure 5 shows the IR spectra of TCE adsorbed on TiO_2 surfaces before and after UV irradiation at 150 K. In these experiments, TCE was first condensed onto the TiO_2 surface at 150 K, then gaseous O_2 was introduced into the cell. After TCE was condensed on the surface, we observed infrared bands at 3161 and 3077 cm^{-1}

(31) Kraeutler, B.; Bard, A. J. *J. Am. Chem. Soc.* **1978**, *100*, 5985.
(32) Tang, H.; Berger, H.; Schmid, P. E.; Levy, F. *Solid State Commun.* **1994**, *92*, 267.
(33) Herzberg, G. *Molecular Spectra and Molecular Structure II, Infrared and Raman Spectra of Polyatomic Molecules*; D. van Nostrand: Princeton, 1945.
(34) Berney, C. V.; Eggers, D. F., Jr. *J. Chem. Phys.* **1964**, *40*, 990.
(35) Chackerian, C., Jr.; Eggers, D. F., Jr. *J. Chem. Phys.* **1965**, *43*, 757.
(36) *The Merck Index, An Encyclopedia of Chemicals, Drugs, and Biologicals*; 11th ed.; Budavari, S., O'Neil, M. J., Smith, A., Heckelman, P. E., Eds.; Merck & Co., Inc.: Rahway, 1989.

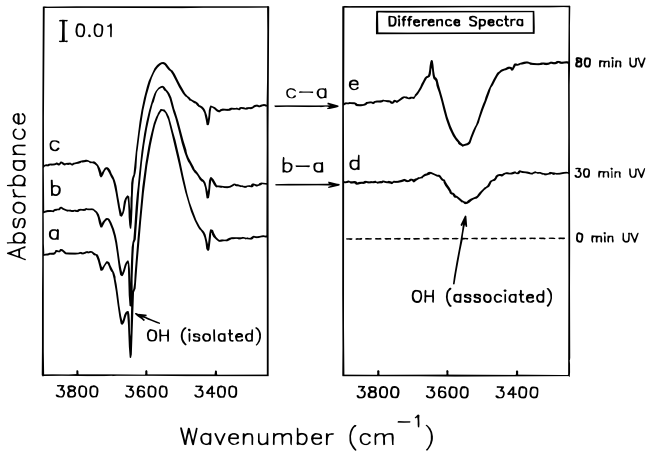

Figure 6. Infrared spectra of the OH stretching region for the photooxidation of TCE at 150 K. The absorption spectra are shown at the left, and the corresponding difference spectra are shown on the right. The left-hand spectra have been ratioed against the spectrum obtained prior to TCE adsorption, clearly showing the conversion of isolated hydroxyl groups to associated hydroxyl groups by TCE adsorption; this process is reversed on photooxidation.

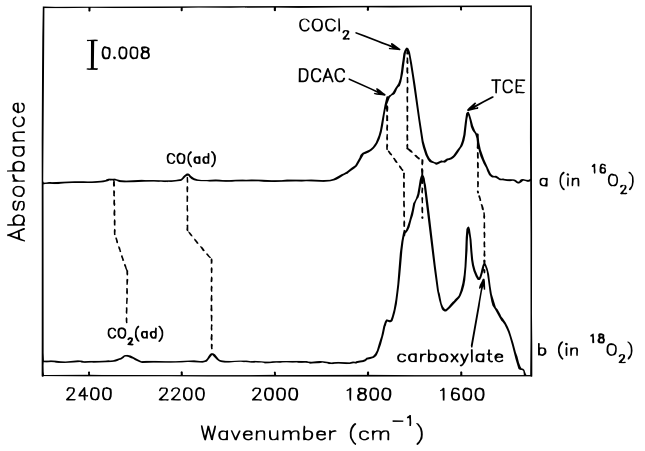

Figure 7. Isotopic shifts of carbonyl stretching frequencies of photolytically generated adsorbed species from TCE oxidation on TiO_2 at 150 K in $^{16}O_2$ and $^{18}O_2$.

for TCE (the symmetric and asymmetric C−H stretch modes), at 1589 cm^{-1} for the C═C stretch, at 1246 cm^{-1} for the CH−Cl bend, and at 1090 cm^{-1} for the C−Cl stretch, based on the assignment for gas-phase TCE.[12] After UV irradiation for ∼30 min, Figure 5b shows new multiple infrared features in the 1600−1800-cm^{-1} region with a peak at 1737 cm^{-1}. There was also an increase in intensity in the band at 1090 cm^{-1}. Based on a separate experiment using pure DCAC, the newly formed bands in Figure 5b are assigned to DCAC. Figure 5c shows the infrared spectrum after a total UV irradiation of ∼80 min; we observed further growth of the band at 1737 cm^{-1} due to continued DCAC production, and a relatively large increase in the shoulder band at 1719 cm^{-1} due to $COCl_2$ production. At the same time, we observed development of a shoulder peak at 1570 cm^{-1} and a new peak at 1225 cm^{-1}, and further increase in the intensity of the band at 1090 cm^{-1}. We assign those newly developed bands at 1719, 1225, and 1090 cm^{-1} to $COCl_2$ adsorbed on TiO_2. The shoulder at 1570 cm^{-1} is tentatively assigned to surface carboxylate species and will be discussed later.[37]

The insert of Figure 5 shows the kinetics of TCE oxidation on the TiO_2 surface at 150 K. It shows that the rate of loss of TCE decreases with time and the oxidation reaction essentially stops after 40 min of UV irradiation. The insert also shows that ∼30% of the TCE is still unreacted after 80 min of UV irradiation. The termination of the photooxidation was not due to lack of oxygen since we observed that the TCE was completely oxidized after heating up the TiO_2 to 300 K to vaporize adsorbed species and performing the gas-phase photooxidation at 300 K as in previous experiments. The experiments shown in Figure 5 which involve the presence of adsorbed layers on TiO_2 at 150 K yield very small levels of TCE oxidation compared to the gas-phase experiments at 300 K.

Figure 6 shows the infrared spectral changes in the OH stretching region during the photooxidation of TCE on the TiO_2 surface at 150 K. In the absorption spectra shown in the left panel, spectrum (a) was obtained before any UV irradiation, spectrum (b) was obtained after 30 min of UV irradiation, and spectrum (c) was obtained after a total of 80 min of UV irradiation. The broad peak at ∼3550 cm^{-1} corresponds to the associated OH groups interacting with TCE on the surface. The infrared peaks at ∼3700 cm^{-1} are due to isolated OH groups. The negative infrared absorption of the isolated OH groups results from ratioing of sample transmittance containing adsorbed TCE with that of the background without TCE, indicating loss of isolated OH groups after adsorption of TCE onto the TiO_2 surface. The difference spectra are shown in the right panel of Figure 6. Spectrum 6d is obtained by subtracting spectrum 6a from 6b, and spectrum 6e by subtracting spectrum 6a from 6c. The difference spectra show that the intensity of the associated OH stretches decreased and the intensity of the isolated OH stretches increased during UV irradiation, suggesting that isolated OH groups on the surface were regenerated from associated OH groups during the photooxidation due to consumption of adsorbed TCE. This is not surprising since a similar phenomenon was also observed on other oxide surfaces.[38] However, Figure 6 illustrates a very important point that the hydroxyl groups on the TiO_2 surface were not consumed in the photooxidation process.

Figure 7 shows the infrared spectra of surface species following partial TCE oxidation (as an adsorbed species) on TiO_2 using oxygen-18 at 150 K. The result using oxygen-16 is also shown for the purpose of comparison. In the oxidation using oxygen-16, in Figure 7a, we observed multiple bands in the 1600−1800-cm^{-1} region, and a shoulder at 1570 cm^{-1} which we assigned to the carbonyl stretches of DCAC, $COCl_2$, and surface carboxylate groups, respectively. The band at 1589 cm^{-1} is the C═C stretch of TCE which remains on the TiO_2 surface after partial oxidation. When oxygen-18 is used, Figure 7b shows that the carbonyl stretches of DCAC and $COCl_2$ at ∼1800 cm^{-1} are shifted ∼35 cm^{-1} to lower wavenumbers, and the shoulder at ∼1570 cm^{-1} of the surface carboxylate is also shifted to 1551 cm^{-1}. The isotopic shifting we observed in Figure 7 is consistent with our assignments of those bands to carbonyl stretches of DCAC, $COCl_2$, and surface carboxylate species. The shifts upon using oxygen-18 indicate that $^{18}O_2$ in the gas phase is involved in the oxidation of TCE to DCAC, $COCl_2$, and carboxylate species on the TiO_2 surface. This isotopic result is the same as we saw in Figure 4 for the gas-phase photoreaction at room temperature. Figure 7 also shows that the IR spectra of adsorbed CO and CO_2 are also shifted upon using oxygen-18, showing that oxygen from the gas phase was also involved in the production of those small quantities of CO and CO_2.

(37) Nakamoto, K. *Infrared and Raman Spectra of Inorganic and Coordination Compounds*, 4th ed.; John Wiley & Sons: New York, 1986.

(38) Beebe, T. P., Jr.; Crowell, J. E.; Yates, J. T., Jr. *J. Phys. Chem.* **1988**, *92*, 1296.

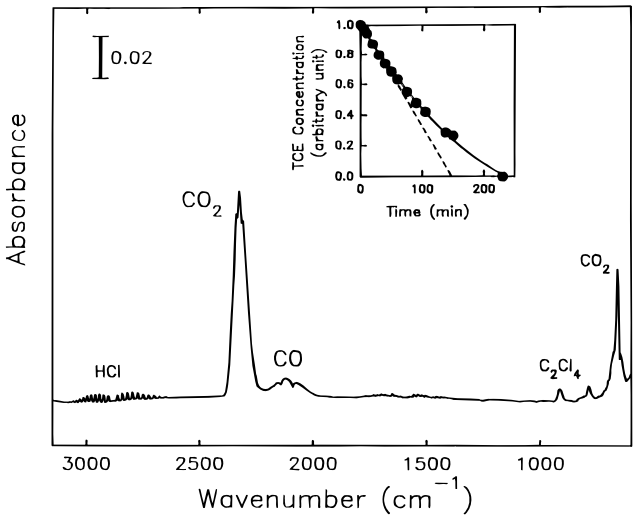

Figure 8. Gas-phase infrared spectrum obtained after photooxidation of TCE at 473 K in $^{18}O_2$ for 365 min. The insert shows the change of TCE concentration with reaction time based on infrared measurements.

C. Photooxidation and Thermal Oxidation at 473 K. The degree of involvement of thermal processes in the sequence of steps observed in the photooxidation of TCE at 300 K was investigated by carrying out similar measurements at 473 K. Figure 8 shows the infrared spectrum obtained after photooxidation of TCE at 473 K using $^{18}O_2$ for 365 min. It can be seen that $COCl_2$ is absent in the spectrum and only CO_2, CO, HCl, and a small quantity of tetrachloroethylene, C_2Cl_4, are observable in the gas phase. The presence of C_2Cl_4 is indicated by the small bands at 912 and 780 cm^{-1}. Control experiments indicate that no thermal reaction occurs between TCE and O_2 at 473 K over TiO_2. Thus TCE is only photooxidized at 473 K. In a control experiment, we found that $COCl_2$ reacts rapidly with TiO_2 at 473 K by means of a thermal process, giving C_2Cl_4 in the gas phase in the presence of O_2(g).

The insert of Figure 8 shows the kinetics of TCE consumption in the photooxidation at 473 K. The gradual decrease in the slope of the TCE consumption curve clearly suggests that the rate of TCE consumption decreases with reaction time, which is in contrast to the results observed in the oxidation carried out at 300 K.

IV. Discussion

A. Band Gap Excitation for TiO_2-Source of Activation for TCE Photooxidation. The band gap of rutile-TiO_2 is near 3.02 eV while for anatase-TiO_2 the band gap is 3.2 eV.[31,32] The powdered TiO_2 used in this work consists of a mixture of anatase (70%) and rutile (30%), and exhibits a photooxidation threshold for TCE near 3.1 eV, as shown in Figure 3. This is consistent with the band gaps of anatase and rutile, and within the error of the experimental measurements.

An alternative view, involving a photochemical radical chain mechanism, is not supported by these results. The UV absorption threshold for TCE is at ~4.5 eV,[39] far above the 3.1-eV experimental threshold observed here.

Both O_2 and TiO_2 are necessary for the photooxidation of TCE, in accordance with previous studies.[14−16,21] TiO_2 lattice oxygen is excluded from involvement in the photochemistry, except in an isotopic exchange process with the final product, CO_2. This oxygen isotopic exchange process probably involves a carboxylate species which was observed on the surface following TCE photooxidation.

(39) Hubrich, C.; Stuhl, F. *J. Photochem.* **1980**, *12*, 93.

B. Sequence of Photooxidation Reactions. The overall reactions observed here may be written as in eqs 2−7:

$$CHCl{=}CCl_2(g) \xrightarrow{TiO_2} CHCl{=}CCl_2(a) \quad (2)$$

$$O_2(g) \xrightarrow{TiO_2} O_2(a) \quad (3)$$

$$O_2(a) + h\nu \xrightarrow{TiO_2} O^*_2(a) \quad (4)$$

$$^1/_2O^*_2(a) + CHCl{=}CCl_2(a) \xrightarrow{TiO_2} Cl_2CH{-}COCl(a) \quad (5)$$

$$Cl_2CH{-}COCl(a) \overset{TiO_2}{\leftrightarrow} Cl_2CH{-}COCl(g) \quad (6)$$

$$Cl_2CH{-}COCl(a) + O^*_2(a) \xrightarrow{TiO_2} \ldots Cl_2CO(g) + CO(g) + CO_2(g) + HCl(g) + CHCl_3(g)(\text{trace}) \quad (7)$$

The stoichiometry of reaction 7 with respect to carbon and oxygen could be determined from our experiments as approximately

$$CHCl_2COCl + 1.17O_2(a) \rightarrow 0.38Cl_2CO + 0.28CO + 1.34CO_2 \quad (8)$$

In addition, we have observed the thermal reaction at 473 K:[26]

$$2Cl_2CO(g) + TiO_2(\text{reduced}) \xrightarrow[O_2]{473\ K} C_2Cl_4(g) + TiO_2(\text{oxidized}) \quad (9)$$

The constant slope observed in Figure 2 for TCE may be attributed to the electron-transfer kinetics for electrons from the TiO_2 surface to a saturated layer of adsorbed O_2, as discussed by Gerischer for O_2 on TiO_2,[4] and by Tanaka and Blyholder[30] for CO oxidation on ZnO. It is suggested that the electron-transfer step (eq 4) is the rate-controlling step. This will give apparent zero-order kinetics for TCE under conditions where a saturated layer of TCE is present.

The observation of $CHCl_3$ suggests that a side reaction was also occurring along with the oxidation reaction. The formation of $CHCl_3$ was also reported by Sanhueza and Heicklen[40] in the reaction of $O(^3P)$ with TCE, and by Huybrechts and Meyers[41] in the gas-phase chlorine-photosensitized oxidation of TCE. However, in the chlorine-photosensitized oxidation, trichloroethylene epoxide and CCl_4 were also formed. The fact that we only observed $CHCl_3$ suggests that $CHCl_3$ was formed through $O(^3P)$. The origin of $O(^3P)$ may be due to the following mechanism, as suggested by Teichner and Formenti.[42]

$$O_2(a) + e^- \rightarrow O_2^-(a) \quad (10)$$

$$O_2^-(a) + h^+ \rightarrow 2O^*(a) \quad (11)$$

C. Comparison of the Photooxidation of TCE at Various Temperatures. The two experiments at 150 and 300 K are very informative for understanding the photooxidation of TCE. At 300 K, the coverage of adsorbed TCE in equilibrium with TCE(g) is expected to be small in comparison to experiment at

(40) Sanhueza, E.; Heicklen, J. *Int. J. Chem. Kinet.* **1974**, *6*, 553.
(41) Huybrechts, G.; Meyers, L. *Trans. Faraday Soc.* **1966**, *62*, 2191.
(42) Teichner, S. J.; Formenti, M. Heterogeneous Photocatalysis. In *Photoelectrochemistry, Photocatalysis and Photoreactors, Fundamentals and Developments*, Series C; Schiavello, M., Ed.; D. Reidel Publishing Company: Dordrecht, The Netherlands, 1984; Vol. 146, pp 457−489.

150 K where a condensed layer of TCE is produced. Two large differences in behavior were noted under these two conditions:

(1) At 300 K, complete consumption of TCE occurred to produce $COCl_2$, CO, CO_2, HCl, and $CHCl_3$.

(2) At 150 K, incomplete reaction occurred for equivalent quantities of TCE, O_2, and TiO_2 and a similar UV fluence.

This comparison suggests that site blocking occurs under conditions where the condensed layer of TCE is present. It is likely that TCE blocks access of O_2(g) to the surface sites necessary for addition of O_2 by the photoprocess. In addition, photoproducts such as $COCl_2$ may also block sites needed by O_2, turning off the photooxidation process as seen in Figure 5.

The isotopic results are the same for the experiments at 150 and 300 K. In both cases, only the oxygen from the gas-phase molecular O_2 was observed to be incorporated in the reaction intermediates.

D. Role of H_2O in the Photooxidation of TCE. Practical photooxidation reactions are often carried out in the presence of water. Therefore in Figure 4 we carried out the photooxidation of TCE with $^{18}O_2$ in the presence of $H_2{}^{16}O$(g). The infrared spectra of the gas proucts indicate that $H_2{}^{16}O$ is ineffective in incorporating oxygen-16 into the intermediate (DCAC) or into the final products (CO and Cl_2CO). *This and the fact that surface hydroxyl groups were not consumed during photooxidation, as shown in Figure 6, provide compelling evidence that surface hydroxyl groups are not involved in the photooxidation of TCE, in contrast with mechanisms postulated in other studies.*[12,21] The results of Figure 4 also indicate that H_2O causes an enhancement of the CO_2 yield and a decrease in the level of DCAC and $COCl_2$ observed as intermediate species. This is probably due to reactions of water with DCAC and $COCl_2$.[19,36]

The lack of oxygen-16 incorporation from water into the photooxidation products indicates that mechanisms involving $OH^{\bullet}$ species as oxidizing agents[3,20,21] are probably inoperative in TCE photooxidation over TiO_2, consistent with recent studies of CH_3Cl photooxidation over TiO_2(110).[5] These observations exclude, at the sensitivity limits of our measurements, the involvement of processes like

$$H_2O + h^+ \rightarrow OH^{\bullet} + H^+ \qquad (12)$$

as postulated by others.[1,3,6,9,43,44]

V. Summary of Results

The kinetics and product sequence for the photooxidation of trichloroethylene (TCE) on powdered TiO_2 have been studied using infrared spectroscopy, in separate experiments where little background water (or surface hydroxyls) is present or alternatively where large amounts of background water are employed.

The following results have been obtained:

(1) TCE is photooxidized on TiO_2 by electronically activated chemisorbed O_2. All oxidation products originate from O_2 rather than lattice oxygen in TiO_2, with the exception of the CO_2 product which probably exchanges oxygen atoms with lattice oxygen via a surface carboxylate species.

(2) The photothreshold for photooxidation of TCE on TiO_2 is near 3.1 eV, indicative of band gap excitation in TiO_2 leading to O_2 excitation by electron-hole pair excitation in the TiO_2 and thereby to the photocatalytic oxidation process.

(3) A sequence of chemical steps are observed in the photooxidation of TCE, which first photooxidizes to $Cl_2HC-COCl$ (DCAC). Subsequent continued photooxidation produces Cl_2CO, CO, CO_2, HCl, and $CHCl_3$ at 300 K.

(4) At 473 K, a thermal reaction converting Cl_2CO to $Cl_2C{=}CCl_2$ on TiO_2 is observed. This molecule then undergoes photooxidation itself.

(5) Evidence is presented showing that at 150 K, the adsorption of TCE (and possibly the photooxidation products of TCE) is able to retard the photooxidation process possibly by blockage of sites for O_2 adsorption.

(6) The isotopic labeling of products in the photooxidation of TCE to DCAC, Cl_2CO, CO, and CO_2 is uninfluenced by the presence of isotopically labeled H_2O. This indicates that mechanisms involving $OH^{\bullet}$ as an oxidizing agent are unlikely.

Acknowledgment. We acknowledge with thanks the Army Research Office for financial support.

JA952155Q

(43) Okamoto, K.; Yamamoto, Y.; Tanaka, H.; Tanaka, M. *Bull Chem. Soc. Jpn.* **1985**, *58*, 2015.

(44) Blake, D. M.; Webb, J.; Turchi, C.; Magrini, K. *Solar Energy Mater.* **1991**, *24*, 584.

(45) Miyake, A.; Nakagawa, I.; Miyazawa, T.; Ichishima, I.; Shimanouchi, T.; Mizushima, S. *Spectrochim. Acta* **1958**, *13*, 161.

(46) Hannus, I.; Kiricsi, I.; Tasi, Gy; Fejes, P. *Appl. Catal.* **1990**, *66*, L7.